Electric-field effects on the charge-transfer excitation in quasi-one-dimensional halogen-bridged mixed-valence Pt complexes: [Pt(ethylenediamine)$_2$] [Pt(ethylenediamine)$_2X_2$](ClO$_4$)$_4$ (X=Cl,Br,I)

Yoshiki Wada
National Institute for Research in Inorganic Materials, Tsukuba 305, Japan

Masahiro Yamashita
College of General Education, Nagoya University, Nagoya 464-01, Japan
(Received 12 April 1990)

The electroreflectance spectra of the halogen-bridged mixed-valence Pt complexes, [Pt(ethylenediamine)$_2$][Pt(ethylenediamine)$_2X_2$](ClO$_4$)$_4$ (X=Cl, Br, and I), have been measured. Electric-field-induced new absorption bands that can be assigned to optically forbidden charge-transfer (CT) excitons with even parity have been found at a little higher energy than the optically allowed CT excitons with odd parity. The modulation mechanism can be quantitatively explained by the electric-field-induced mixing between the odd and the even CT excitons. The energy separations between the odd and the even excitons of the X=Cl, Br, and I complexes are 0.54, 0.46, and 0.24 eV, respectively. This indicates the large electron-hole attractive energies in the complexes. The halogen-dependent change of the energy separations can be explained in terms of the intersite electron transfer energies.

I. INTRODUCTION

The halogen-bridged mixed-valence metal complex (HMMC) has been studied as a typical material for studies of photoexcited states and their relaxation processes in a one-dimensional electron system. The complex is represented as $(MA_2)(MA_2X_2)Y_4$, where M denotes a metal atom (Pt, Pd, or Ni), X a halogen atom (Cl, Br, or I), A a ligand molecule, and Y a counteranion. The HMMC has a linear chain structure of metal and halogen ions, as shown in Fig. 1.[1] Charge-density waves (CDW's) with periods of twice the metal-metal distance are caused by halogen-ion distortion from the midpoint between two neighboring metal ions in complexes where M=Pt and Pd. Accordingly, the one-dimensional half-filled conduction band composed of d_{z^2} electrons of the metal ions splits into a valence and a conduction band.[2] On the other hand, some Ni complexes have no halogen-ion distortion and have energy gaps due to electron correlation.[3]

The characteristic feature of HMMC's is that physical properties such as the phase of the ground state, the width of the energy gap, and the amplitude of the halogen distortion can be systematically changed over a wide range by the change of constituent metal and halogen ions.[4,5] Such metal- and halogen-dependent changes are well explained by an extended Peierls-Hubbard model considering the electron-phonon interaction energy S, the transfer energy of an electron between neighboring metal sites T, and the intra- and intersite electron-electron repulsive energies U and V.[6] According to this model, physical properties of HMMC's are determined by cooperation and competition among T, S, U, and V. The metal- and halogen-ion-dependent change of the properties can be explained by the change of S, T, and U. Although electron-electron long-range Coulomb interaction is taken into account as a parameter V, the contribution of V is not apparent in this case. Nevertheless, long-range Coulomb interaction is thought to play a very important role in the determination of the structures of photoexcited states,[6,7] such as excitons and free-electron-hole pairs, and in that of their relaxation processes to the ground state, to self-trapped excitons,[5,6,8–11] to polaron pairs,[12–15] and to soliton pairs,[12,16–19] because Coulomb interaction acts as the binding force between the photogenerated electron and hole.

In the HMMC (M=Pt and Pd), a charge-transfer (CT) excitation causes an intense broad absorption band[5,8,20–24] with an asymmetric-Lorentzian-like line shape[5] for light polarized along the chain axis. The CT excitation originates in the electron-transfer excitation from an $M^{3-\rho}$ ion to a neighboring $M^{3+\rho}$ ion—in other words, electron excitation over the CDW gap. Since no definite fine structure, as is observed in common inorganic semiconductors and insulators, can be observed in the absorption band, it cannot be clarified only from the line shape whether this band is due to the CT exciton or to the interband transition. In previous papers we have interpreted the absorption band in the HMMC as CT exciton absorption[5,25] considering the existence of the intense luminescence band from the self-trapped exciton

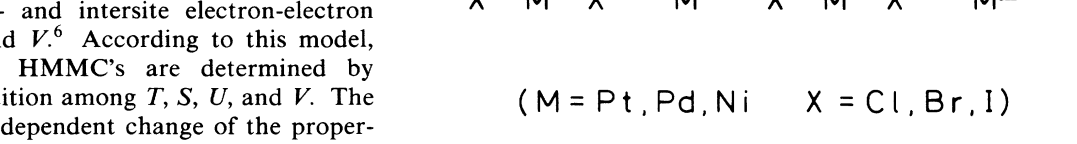

FIG. 1. Linear chain structure of the HMMC. Here, ρ is the deviation of the valency from 3, $0 \le \rho < 1$).

state,[5,8,9] the absence of photoconductivity,[26] and the unusually large oscillatory strength.[5,25] On the other hand, an alternative assignment in which the absorption band is due to the interband transition has been also proposed.[7,24,27] These different interpretations are based on different estimations of the contribution of the long-range Coulomb interaction in the HMMC: it is considered to be large in the exciton interpretation and negligibly small in the interband interpretation.

Electric-field-modulation measurements comprise a useful method for extracting detailed information from absorption bands. By these measurements, hidden electronic states have been found in polydiacetylenes.[28–30] In order to clarify the identity of the absorption band and to get information on the electron-electron Coulomb interaction, we have measured the electroreflectance (ER) spectra of $[Pt(en)_2][Pt(en)_2X_2](ClO_4)_4$, where X = Cl, Br, and I, and en = ethylenediamine; preliminary results from the X = Cl and Br complexes have been briefly reported elsewhere.[31] For simplicity, these materials are abbreviated hereafter as Pt-Cl, Pt-Br, and Pt-I. The modulation mechanism is quantitatively explained by the field-induced mixing between the optically allowed CT exciton and the forbidden CT exciton, which has been found to be an electric-field-induced absorption band in the modulation spectra. The energy separation between the allowed and the forbidden exciton decreases with substitution of the halogen ion in the order Cl, Br, and I. This is thought to correspond to the decrease of the binding energy of the CT exciton due to the increment in the transfer energy (T).

II. EXPERIMENT

The compounds Pt-Cl, Pt-Br, and Pt-I were synthesized by the method previously reported.[32] Single crystals of the compounds were grown from water solution containing 3 wt. % perchloric acid ($HClO_4$) by slow evaporation. Two electrodes with constant aperture width ($\sim$0.2–0.3 mm) between them were formed on a surface of a crystal by painting with silver paste. The sample was immersed in liquid nitrogen. An ac electric field of f = 1 kHz or 200 Hz was applied between the electrodes. A 150-W Xe lamp and a 50-W W lamp were used as light sources. Polarized monochromatic light was obtained by a monochromator and by a Glan-Thompson prism. The crystal aperture was irradiated and the reflected light was detected by photomultiplier tubes or by a PbS photodetector. The signal was fed to a lock-in amplifier. Since the crystals of these complexes have inversion symmetry, the $2f$ component of the field-induced change of the reflectivity was measured. When photomultipliers were used, the frequency of the applied electric field was 1 kHz. On the other hand, when the PbS photodetector was used, the frequency was 200 Hz due to its slow time response.

The ER spectra of Pt-Br were measured with the applied field parallel and perpendicular to the chain axis and with the light polarization parallel and perpendicular to the chain axis in the wavelength range $\sim$350–1120 nm using photomultiplier tubes. The ER spectra of Pt-Cl were measured with the applied field parallel to the chain axis and with the light polarization parallel and perpendicular to the chain axis in the wavelength range of $\sim$280–730 nm using photomultiplier tubes. The ER spectra of Pt-I were measured with the applied field parallel to the chain axis and with the light polarization parallel and perpendicular to the chain axis in the wavelength range $\sim$350–1100 nm using photomultiplier tubes and in the wavelength range $\sim$690–1800 nm using the PbS photodetector. In the wavelength range $\sim$690–1100 nm no difference has been observed between the ER spectra measured by the PbS photodetector (f = 200 Hz) and those measured by photomultiplier tubes (f = 1 kHz). Therefore, the electroreflectance spectra measured for the different applied field frequencies can be connected.

We have also measured the polarized reflectivity spectra of Pt-Cl, Pt-Br, and Pt-I for the wavelength ranges $\sim$195–1100 nm, $\sim$195–1400 nm, and $\sim$195–2400 nm, respectively. The imaginary parts of the dielectric constants ϵ_2 and the modulation spectra of ϵ_2 ($\Delta\epsilon_2$) of these complexes have been obtained from the reflection spectra and the ER spectra by Kramers-Kronig transformation.

III. RESULTS

The polarized reflection spectra of Pt-Br in liquid N_2 are shown in Fig. 2(a). The component polarized along the chain axis is represented by the solid line and that polarized perpendicular to the chain axis is represented by

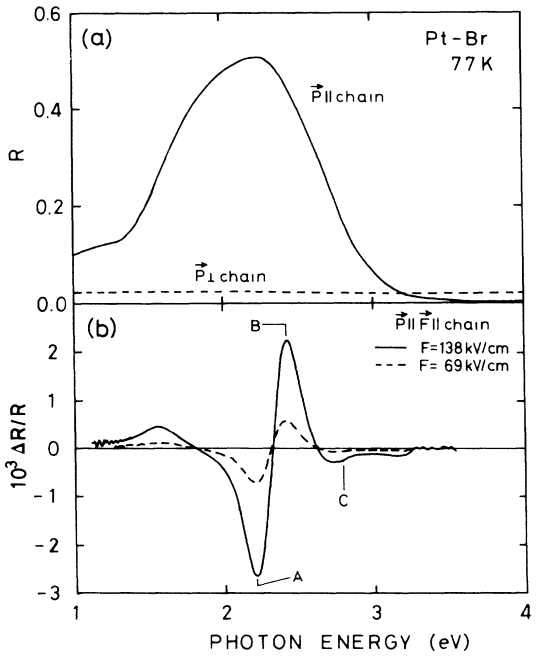

FIG. 2. (a) Polarized reflection spectra of Pt-Br in liquid N_2 parallel to the chain axis (solid line) and perpendicular to the chain axis (dashed line). (b) Polarized electroreflectance spectra in liquid N_2 parallel to the chain axis for the applied electric field parallel to the chain axis. The amplitudes of the applied field are 69 kV/cm (dashed line) and 138 keV/cm (solid line).

the dashed line. The broad large structure which is observed around 2 eV only for the component along the chain axis (solid line) in the figure is caused by the CT excitation. The ER spectra (the amplitudes of the $2f$ components of the field-induced reflectivity change) of Pt-Br in liquid N_2 are also shown in Fig. 2(b). These are the components with the applied electric field parallel to the chain axis and with the light polarization parallel to the chain axis. The amplitudes (half of the peak-to-peak values) of the applied ac electric field (F) are 69 kV/cm (dashed line) and 138 kV/cm (solid line). When the applied field or the light polarization was perpendicular to the chain axis, no signal larger than 10^{-4} was observed up to $F=150$ kV/cm. This is consistent with the one-dimensional electronic structure of the HMMC.

It is clearly seen in Fig. 2(b) that there is no definite energy shift of the structures in the ER spectra by the increment of the amplitudes of applied field by a factor 2. In Fig. 3 the amplitude of the ER signal ($\Delta R/R$) of Pt-Br at the energies indicated by A, B, and C in Fig. 2(b) is plotted versus the amplitudes of the applied field. The points fall on straight lines with slope 2, allowing for some small deviation. This shows that the quadratic dependence of the ER signal amplitude on the amplitude of the applied field is dominant. In Figs. 4(a) and 5(a) the components of the polarized reflection spectra parallel to the chain axes of Pt-Cl and Pt-I, respectively, are shown. In Figs. 4(b) and 5(b), ER spectra of Pt-Cl and Pt-I, respectively, for the applied field parallel to the chain axis and for the light polarization parallel to the chain axis are shown. No signal larger than 10^{-4} was observed in the components polarized perpendicular to the chain axis up to $F=150$ kV/cm. These spectra are quite similar to those of Pt-Br. The ER signals of Pt-Cl and Pt-I also have quadratic electric field dependence.

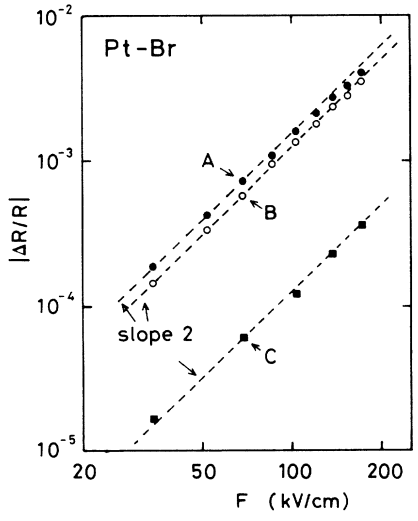

FIG. 3. Relation between the electric-field-induced reflectivity change ($\Delta R/R$) and the amplitude of the applied electric field for the energy points A (2.21 eV), B (2.42 V), and C (2.79 eV).

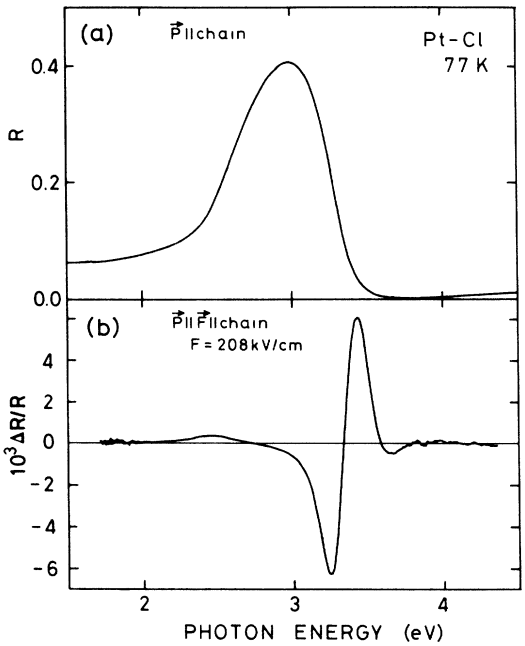

FIG. 4. (a) Polarized reflection spectra of Pt-Cl in liquid N_2 parallel to the chain axis (solid line). (b) Polarized electroreflectance spectra in liquid N_2 parallel to the chain axis for the applied electric field ($F=208$ kV/cm) parallel to the chain axis.

In Fig. 6(a) the imaginary part of the dielectric constant of Pt-Br for polarized light parallel to the chain axis is shown. The intense absorption band at 1.77 eV is the CT excitation absorption band mentioned before. In Fig. 6(b) modulation spectra of ϵ_2 ($\Delta\epsilon_2$) of Pt-Br for the light

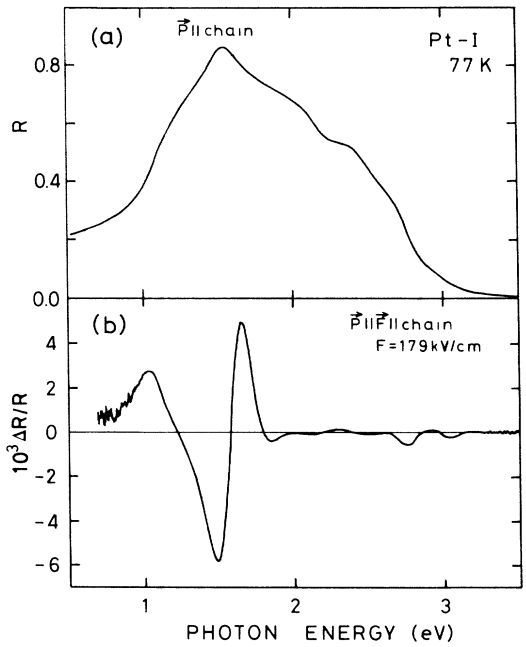

FIG. 5. (a) Polarized reflection spectra of Pt-I in liquid N_2 parallel to the chain axis (solid line). (b) Polarized electroreflectance spectra in liquid N_2 parallel to the chain axis for the applied electric field ($F=179$ kV/cm) parallel to the chain axis.

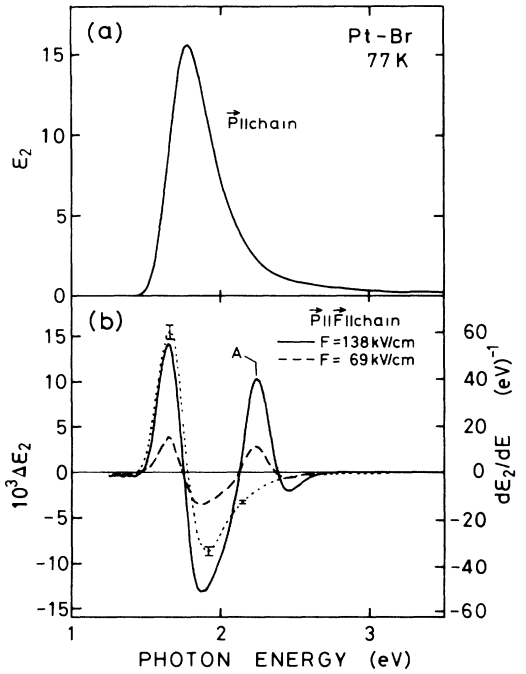

FIG. 6. (a) Imaginary part of the dielectric constant of Pt-Br for the polarization parallel to the chain axis. (b) Modulation spectra and energy derivative of the imaginary part of the dielectric constant (dotted line) of Pt-Br for the light polarization parallel to the chain axis. Here, the applied electric field is parallel to the chain axis and its amplitudes are $F=69$ kV/cm (dashed line) and $F=138$ kV/cm (solid line).

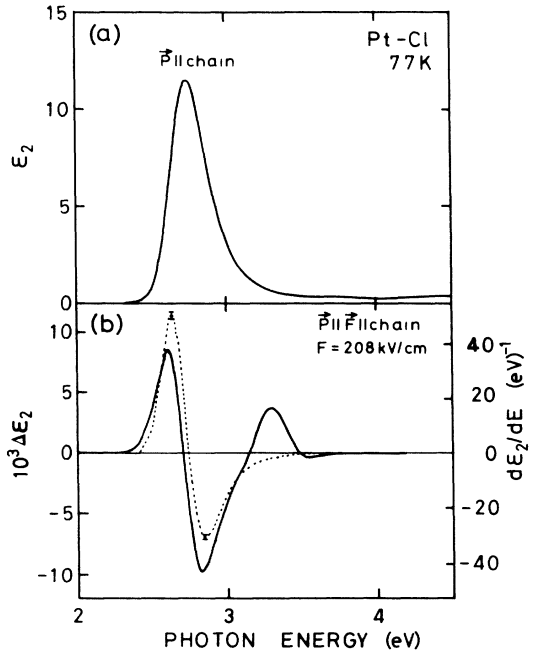

FIG. 7. (a) Imaginary part of the dielectric constant of Pt-Cl for the polarization parallel to the chain axis. (b) Modulation spectra (solid line) and energy derivative of the imaginary part of the dielectric constant (dotted line) of Pt-Cl for the light polarization parallel to the chain axis. Here, the applied electric field ($F=208$ kV/cm) is parallel to the chain axis.

polarization parallel to the chain axis and for applied field parallel to the chain axis are shown: $F=69$ kV/cm (dashed line) and $F=138$ kV/cm (solid line). These values have been obtained by Kramers-Kronig transformation from the reflectivity (R) and ER ($\Delta R/R$) spectra shown in Figs. 2(a) and 2(b). It is readily seen in Fig. 6(b) that there is no definite energy shift of the structures by the increment of the applied electric field strength by a factor 2. This is quite different from the electric field dependence expected from the Franz-Keldysh effect,[33,34] as observed around the interband transition absorption edge in common three-dimensional semiconductors. If the modulation mechanism is the Franz-Keldysh effect, the energy intervals of the points where $\Delta\epsilon_2$ spectra cross 0 must be proportional to $F^{2/3}$, and an obvious electric-field-amplitude-dependent energy shift of the structures must be observed. Thus modulation mechanism cannot be such an effect. The modulation spectra are rather complicated, but it was found that they are quite similar to the spectra of the energy derivative of ϵ_2, $d\epsilon_2/dE$, represented by dotted lines in Fig. 6(b), except for the structures indicated by A. This indicates that the modulation spectra are mainly determined by the energy shift of the allowed CT excitation absorption band to lower energy and the appearance of a field-induced new absorption band at 2.23 eV, indicated by A. Quite similar modulation spectra, which also have quadratic electric field dependence, have been found in polydiace-

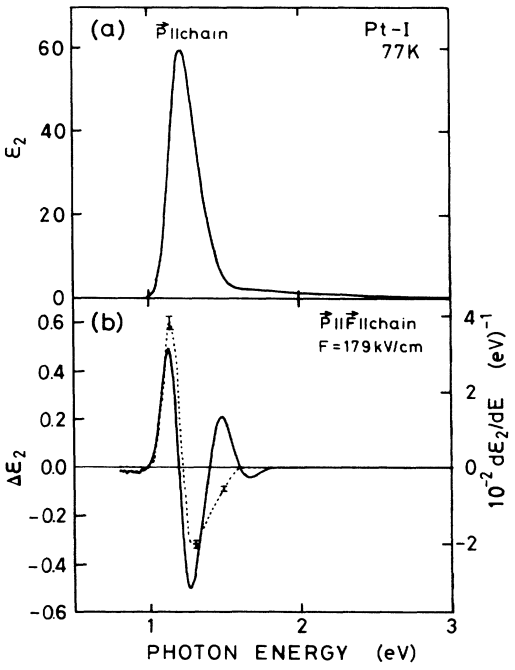

FIG. 8. (a) Imaginary part of the dielectric constant of Pt-I for the polarization parallel to the chain axis. (b) Modulation spectra (solid line) and energy derivative of the imaginary part of the dielectric constant (dotted lines) of Pt-I for the light polarization parallel to the chain axis. Here, the applied electric field ($F=179$ kV/cm) is parallel to the chain axis.

tylenes.[28,29] In polydiacetylene the modulation mechanism has been quantitatively explained by the field-induced mixing between the optically allowed exciton with odd parity and the forbidden exciton with even parity.[28]

In Figs. 7(a) and 8(a) the imaginary part of the dielectric constant ϵ_2 of Pt-Cl and Pt-I, respectively, for the light polarization parallel to the chain axis is shown. In Figs. 7(b) and 8(b) modulation spectra of ϵ_2 for the polarization parallel to the chain axis and for the applied field parallel to the chain axis (solid line) and the energy derivative of ϵ_2 for the light polarization parallel to the chain axis (dotted line) of Pt-Cl and Pt-I, respectively, are shown. It is readily seen that these spectra are qualitatively the same as those of Pt-Br.

IV. DISCUSSION

In previous papers we have interpreted the intense CT excitation absorption bands as CT exciton absorption bands for the following reasons: (1) the existence of intense luminescence from the self-trapped exciton state suggests a considerable long-range electron-electron Coulomb interaction,[5,8,9] (2) the excitation spectra of photoconductivity rise from an energy higher than the peak energy of the absorption band,[26] and (3) the unusually large oscillator strength (larger than 2 for an *MXMX* unit) which cannot be explained by the interband absorption[27] is well explained by the CT exciton model.[25] According to this interpretation, it may be quite natural to expect the existence of an optically forbidden CT exciton with even parity at an energy slightly higher than the optically allowed CT exciton with odd parity. Therefore, we have assigned the field-induced absorption band to the CT exciton with even parity. On the other hand, an alternative interpretation has been proposed, namely that the CT excitation absorption band is an interband absorption.[7,24,27] This is equivalent to the interpretation that the long-range Coulomb interaction is negligibly small in HMMC's. In such a case, the dominant modulation mechanism must be the Franz-Keldysh effect. As mentioned before, electric field dependence of the modulation signal cannot be explained by such an effect. Therefore, such an interpretation can be excluded.

In order to quantitatively verify the above interpretation and to extract more detailed information, we have made a quantitative analysis according to the formalism of the field-induced mixing between the optically allowed CT exciton with odd parity and the optically forbidden CT exciton with even parity.[28,35] Here, only the electric-field-induced mixing between these two CT excitons is taken into account for simplicity. Since the modulation signal is small ($\Delta R/R < 10^{-2}$) and has quadratic electric field dependence, treatment by the perturbation method may be a good approximation. According to the formalism, the amplitudes of the $2f$ component of the energy shifts of the odd (ΔE_o) and the even (ΔE_e) CT excitons are expressed as

$$\Delta E_o = -\Delta E_e = \frac{e^2F^2r^2\cos^2\theta}{2(E_o - E_e)} . \tag{1}$$

Here, E_o (E_e) denotes the energy of odd (even) CT excitons, r the transition dipole moment between odd and even CT excitons, F the amplitude of the applied electric field, θ the angle between the chain axis and applied field, and e the electron charge. The amplitudes of the $2f$ component of the field-induced charge of the oscillator strengths of the even CT exciton (Δf_e) and that of the odd CT exciton (Δf_o) are expressed as

$$\Delta f_e/f_o = \frac{E_e r^2 e^2 F^2 \cos^2\theta}{2E_o(E_o - E_e)^2} , \tag{2a}$$

$$-\Delta f_o/f_o = \frac{r^2 e^2 F^2 \cos^2\theta}{2(E_o - E_e)^2} . \tag{2b}$$

Here, f_o stands for the oscillator strength of the odd CT exciton. Neglecting the broadening effect, the contribution of the optically allowed odd CT exciton to the modulation spectra of ϵ_2 ($\Delta\epsilon_2^o$) is obtained from Eqs. (1) and (2b) as

$$\Delta\epsilon_2^o = -\left[\frac{d\epsilon_2}{dE} + \frac{\epsilon_2}{E_o - E_e}\right]\Delta E_o . \tag{3}$$

We have fitted Eq. (3) to the modulation spectra, taking ΔE_o as a variable parameter. Here, we have substituted the peak energy of the CT exciton absorption band and that of the electric-field-induced absorption band for E_o and E_e, respectively. The energy-shift values of the odd excitons of Pt-Cl, Pt-Br, and Pt-I in Figs. 7(b), 6(b),

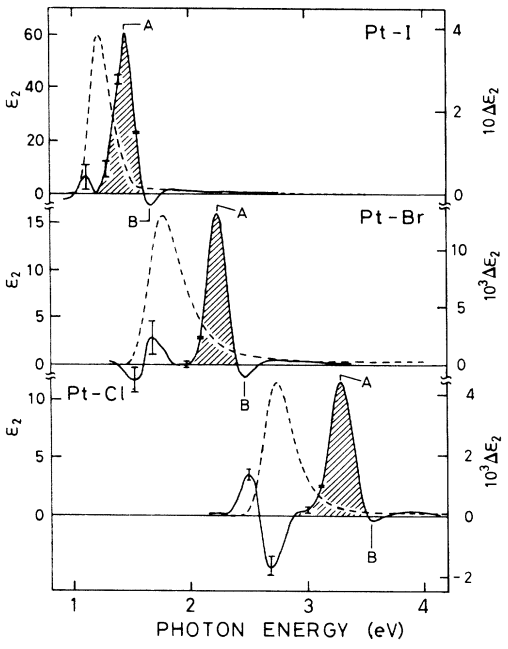

FIG. 9. Difference spectra between the modulation spectra of ϵ_2 ($\Delta\epsilon_2$) and best-fit spectra of $\Delta\epsilon_2^o$ (solid lines) and the imaginary part of the dielectric constant (dashed lines) of Pt-I, Pt-Br, and Pt-Cl for the polarization parallel to the chain axis: $F = 179$ kV/cm and $\Delta E_o = -7.8\times10^{-4}$ eV for Pt-I, $F = 138$ kV/cm and $\Delta E_0 = -1.3\times10^{-4}$ eV for Pt-Br, and $F = 208$ kV/cm and $\Delta E_o = -1.1\times10^{-4}$ eV for Pt-Cl.

TABLE I. Peak energies of the odd CT excitons (E_o), those of field-induced absorption bands (E_e), differences between E_e and E_o ($E_e - E_o$), minimum energies of the structures indicated by B in Fig. 9, and transition dipole moments between odd and even CT excitons obtained from energy shifts (r_s) and those obtained from the induced oscillator strength (r_f).

	E_o (eV)	E_e (eV)	$E_e - E_o$ (eV)	E_b (eV)	r_s (Å)	r_f (Å)
Pt-Cl	2.74	3.28	0.54	3.56	6.3	5.9
Pt-Br	1.77	2.23	0.46	2.47	9.5	8.9
Pt-I	1.22	1.46	0.24	1.67	12.9	12.3

and 8(b), respectively, have been estimated as -1.1×10^{-4} ($F=208$ kV/cm), -1.3×10^{-4} ($F=138$ kV/cm), and -7.8×10^{-4} eV ($F=179$ kV/cm), respectively, within $\pm5\%$ errors. According to Eq. (1), the transition dipole moments of Pt-Cl, and Pt-Br, and Pt-I have been estimated as 6.3, 9.5, and 12.9 Å, respectively, within $\pm5\%$ errors. The difference spectra between $\Delta\epsilon_2$ and the $\Delta\epsilon_2^o$ of Pt-Cl, Pt-Br, and Pt-I are represented by solid lines in Fig. 9, together with the ϵ_2 spectra (dashed line). It is readily seen that the induced absorption bands indicated by A have a simple one-component line shape with half-widths a little narrower than those of the CT exciton absorption bands, which are also represented in these figures (dashed lines). Such narrow bandwidths are consistent with the even-CT exciton picture.

We can also estimate the transition dipole moments from the area of the induced absorption band, indicated by hatching, using Eq. (2a). The transition dipole moments of Pt-Cl, Pt-Br, and Pt-I have been estimated as 5.9, 8.9, and 12.3 Å, respectively, within $\pm10\%$ errors. These values of the transition dipole moments and those estimated from the energy shifts agree sufficiently well with each other. This means that the modulation mechanism is well explained by the simple CT exciton formalism. The peak energies of the CT exciton absorption bands, E_o; those of the induced bands, E_e; transition dipole moments estimated by energy shifts, r_s; and those estimated by induced oscillator strength, r_f, are listed in Table I.

It is easily seen in Table I that the energy separation of these two absorption bands ($E_e - E_o$) decreases with halogen-ion substitution in the order Cl, Br, and I. Such systematic halogen-dependent changes have commonly been found in other fundamental values, such as the amplitudes of the halogen-ion distortion, the exciton peak energies, Stokes-shift energies, and oscillator strengths of the odd excitons.[5] Such halogen dependence has been explained by the increase of the transfer energy T in the order $T(\mathrm{Cl}) < T(\mathrm{Br}) < T(\mathrm{I})$. It seems quite natural to consider that the increase of the transfer energy decreases the binding energy of both even and odd CT excitons including the energy separation between them. It is also seen in Table I that the transition dipole moment r between odd and even excitons increases in the order $r(\mathrm{Cl}) < r(\mathrm{Br}) r < r(\mathrm{I})$. Such an increase of the transition dipole moments may be attributed to the increase of the exciton radius of both the even and odd CT excitons due to the increase of the transfer energy. This is consistent with the decrease of the energy separation $E_e - E_o$. Such large energy separations mean large electron-hole attractive energies. Unfortunately, we cannot estimate the values of the long-range Coulomb interaction energies such as V (electron-electron repulsion energy between nearest-neighbor sites) because little is known about one-dimensional excitons in CDW systems. Nevertheless, it may be safe to consider that the values of V are at least of the same order of magnitude as the value of $E_e - E_o$.

There are small minima indicated by B on the higher-energy side of the induced absorption band: the minimum energies (E_b) are also listed in Table I. The energy separation between the minimum and the even exciton ($\Delta E = E_b - E_e$) decreases with halogen substitution in the order $\Delta E(\mathrm{Cl}) > \Delta E(\mathrm{Br}) > \Delta E(\mathrm{I})$. Such halogen-dependent change is the same as the change of the separation between odd and even excitons mentioned before. However, we limit ourselves to pointing out the existence of such structures because it cannot be distinguished whether these structures correspond to real electronic states or trivial interference structures which are overlooked in the simple CT exciton formalism mentioned before.

ACKNOWLEDGMENTS

We are grateful to Professor K. Nasu and Professor T. Mitani for many enlightening discussions, to Dr. S. Abe for useful comments and discussions, and to Dr. K. Era for useful discussion.

[1]B. M. Craven and D. Hall, Acta. Crystallogr. **14**, 475 (1961).
[2]M. H. Whangbo and M. J. Foshee, Inorg. Chem. **20**, 113 (1981).
[3]K. Toriumi, Y. Wada, T. Mitani, S. Bando, M. Yamashita, and Y. Fujii, J. Am. Chem. Soc. **111**, 2341 (1989).
[4]R. Aoki, Y. Hamaue, S. Kida, M. Yamashita, T. Takemura, Y. Furuta, and A. Kawamori, Mol. Cryst. Liq. Cryst. **81**, 301 (1982).
[5]Y. Wada, T. Mitani, M. Yamashita, and T. Koda, J. Phys. Soc. Jpn. **54**, 3143 (1985).
[6]K. Nasu, J. Phys. Soc. Jpn. **52**, 3865 (1983); **53**, 302 (1984), **53**, 427 (1984).

[7]S. Abe, J. Phys. Soc. Jpn. **58**, 62 (1989).
[8]H. Tanino and K. Kobayashi, J. Phys. Soc. Jpn. **52**, 1446 (1983).
[9]M. Tanaka, S. Kurita, Y. Okada, T. Kojima, and Y. Yamada, Chem. Phys. **96**, 343 (1985).
[10]Y. Wada, K. Era, and M. Yamashita, Solid State Commun. **67**, 953 (1988).
[11]H. Tanino, W. Ruhle, and K. Takahashi, Phys. Rev. B **38**, 12 716 (1988).
[12]D. Baeriswyl and A. R. Bishop, J. Phys. C **21**, 339 (1988).
[13]N. Matsushita, N. Kojima, T. Ban, and I. Tujikawa, J. Phys. Soc. Jpn. **56**, 3808 (1987).
[14]S. Kurita, M. Haruki, and K. Miyagawa, J. Phys. Soc. Jpn. **57**, 1789 (1988).
[15]A. Mishima and K. Nasu, Phys. Rev. B **39**, 5763 (1989).
[16]S. Ichinose, Solid State Commun. **50**, 137 (1984).
[17]Y. Onodera, J. Phys. Soc. Jpn. **56**, 250 (1987).
[18]N. Kuroda, M. Sakai, Y. Nishina, M. Tanaka, and S. Kurita, Phys. Rev. Lett. **58**, 2212 (1987).
[19]A. Mishima and K. Nasu, Phys. Rev. B **39**, 5758 (1989).
[20]S. Yamada and R. Tsuchida, Bull. Chem. Soc. Jpn. **29**, 421 (1956); **29**, 894 (1956).
[21]P. Day, in *Low-Dimensional Cooperative Phenomena,* edited by H. J. Keller (Plenum, New York, 1974), p. 191.
[22]R. J. H. Clark and M. L. Franks, J. Chem. Soc. Dalton Trans. **1977**, 198.
[23]G. C. Papavassiliou and A. D. Zdesis, J. Chem. Soc. Faraday II **76**, 104 (1980).
[24]M. Tanaka, S. Kurita, T. Kojima, and Y. Yamada, Chem. Phys. **91**, 257 (1984).
[25]Y. Wada, T. Mitani, K. Toriumi, and M. Yamashita, J. Phys. Soc. Jpn. **58**, 3013 (1989).
[26]M. Haruki, M. Tanaka, and S. Kurita, Synth. Met. **21**, 373 (1987).
[27]M. Tanaka, S. Kurita, M. Fujisawa, and S. Matsumoto, J. Phys. Soc. Jpn. **54**, 3632 (1985).
[28]Y. Tokura, Y. Oowaki, T. Koda, and R. H. Baughman, Chem. Phys. **88**, 437 (1984).
[29]L. Sebastian and G. Weiser, Phys. Rev. Lett. **46**, 1156 (1981).
[30]L. Sebastian and G. Wieser, Chem. Phys. **62**, 447 (1981).
[31]Y. Wada, T. Mitani, M. Yamashita, and T. Koda, Synth. Met. **19**, 907 (1987).
[32]N. Matsumoto, M. Yamashita, and S. Kida, Bull. Chem. Soc. Jpn. **51**, 2334 (1978).
[33]W. Frantz, Naturforch. **13**, A484 (1958).
[34]L. V. Keldysh, Zh. Eksp. Teor. Fiz. **34**, 1138 (1958) [Sov. Phys.—JETP **7**, 788 (1958)].
[35]D. Haarer, M. R. Philpott, and Morawiz, J. Chem. Phys. **63**, 5238 (1975).